Quantum control of coherent anti-Stokes Raman processes

Dan Oron, Nirit Dudovich, Dvir Yelin, and Yaron Silberberg
Department of Physics of Complex Systems, Weizmann Institute of Science, Rehovot 76100, Israel
(Received 7 May 2001; published 2 April 2002)

Using femtosecond pulse-shaping techniques, we are able to control several useful parameters of coherent anti-Stokes Raman spectroscopy (CARS). By shaping both the pump and the Stokes pulses with an appropriate spectral phase function, we eliminated the nonresonant CARS background. In addition, we designed pulses which selectively excite one of two neighboring Raman levels, even when both are well within the excitation spectrum. High-resolution CARS spectra were recorded in spite of the broad femtosecond pulse spectrum.

DOI: 10.1103/PhysRevA.65.043408 PACS number(s): 32.80.Qk, 42.65.Dr, 78.47.+p, 82.53.Kp

Quantum coherent control consists of interfering different paths of a given system constructively to induce a desirable outcome, while interfering destructively paths leading to other outcomes. Several works have recently presented coherent control of light interaction with matter, using ultrashort pulses and some form of phase manipulation of the different frequency components of the pulse. Weiner *et al.* [1] have demonstrated mode-selective impulsive stimulated Raman scatter. Meshulach *et al.* [2] have demonstrated cancellation of the two-photon absorption process, while Dudovich *et al.* [3] achieved enhancement of a resonant two-photon absorption process. Adaptive shaping [4], a combination of a pulse-shaping apparatus and a closed feedback loop, has been used to compress pulses, to control the branching ratio of chemical reactions [5] and for mode-selective stimulated Raman scattering [6].

In this work, we demonstrate quantum control of coherent anti-Stokes Raman spectroscopy (CARS), the most commonly used nonlinear spectroscopic method. In CARS, a pump and a Stokes beam, centered at ω_p and ω_s, and a probe beam, centered at ω_{pr}, are focused together, generating a signal at a frequency $\omega_p-\omega_s+\omega_{\mathrm{pr}}$. The energy-level diagram of this process is shown in Fig. 1(b). Resonant enhancement of the process occurs when the energy difference $\omega_p-\omega_s$ coincides with a vibrational level of the medium. In many cases, the pump beam is used also as the probe beam, generating a signal at $2\omega_p-\omega_s$. Coherent Raman processes have emerged as an important spectroscopic tool in the past few decades [7], especially in the field of femtosecond time-resolved spectroscopy. For example, Leonhardt *et al.* [8] measured the energy difference and the lifetimes of two (or more) Raman levels by Fourier-decomposing the quantum beats of the CARS signal using femtosecond pulses. Since then, this method has been used extensively to analyze the energy-level diagram of complex molecules. CARS has recently become a favorable method for nonlinear depth-resolved microscopy [9–11]. The femtosecond CARS method, however, suffers from two major drawbacks: a strong nonresonant background signal [12] and lack of selectivity between neighboring energy levels due to the large bandwidth of the pulses. While the former problem can be reduced using a complex polarization arrangement of the three exciting beams [13], the latter can be solved only by coherent control methods.

In this paper, we demonstrate coherent control of the CARS process. We are able to measure Raman spectra with a resolution of the order of 5 cm^{-1} using shaped pulses with a bandwidth of about 120 cm^{-1}. We also demonstrate nearly complete suppression of the nonresonant background signal, which is an unwanted noise term for most spectroscopic and microscopic applications. Finally, we achieve selective population of only one of the two Raman levels of pyridine, both of which lie within the bandwidth of the excitation pulses. All these were obtained using very simple spectral phase manipulations. Simple modeling was used to derive the required spectral phases, and the measured signals agree well with the model predictions.

In most femtosecond CARS experiments, only a small fraction of the population is excited to the vibrational level. Hence, it is justified to use a perturbative approach to analyze this process. The nonlinear polarization driving the CARS signal generated by a three-beam configuration can be approximated by time-dependent perturbation theory as

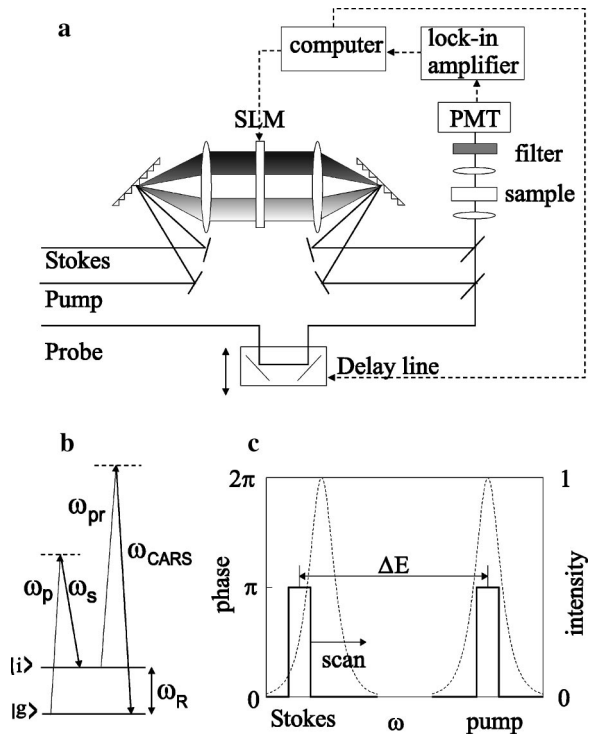

FIG. 1. (a) Outline of the experimental setup. (b) Energy-level diagram of the CARS process. (c) Schematic diagram of the phase function applied on the pump and Stokes beams.

$$P^{(3)}(t) = -\frac{1}{\hbar^3}\sum_{mnl}\mu_{gl}\mu_{ln}\mu_{nm}\mu_{mg}\exp[-(i\omega_{lg}+\Gamma_{lg})t]\int_{-\infty}^{t}dt_1\int_{-\infty}^{t_1}dt_2\int_{-\infty}^{t_2}dt_3$$
$$\times\epsilon_p(t_3)\epsilon_s^*(t_2)\epsilon_{pr}(t_1)\exp[(i\omega_{ln}+\Gamma_{ln})t_1]\exp[(-i\omega_{mn}+\Gamma_{mn})t_2]\exp[(i\omega_{mg}+\Gamma_{mg})t_3], \quad (1)$$

where $|m\rangle$, $|n\rangle$, and $|l\rangle$ are the intermediate levels, μ_{ij} are the dipole moments, and $\omega_{ij}=(E_i-E_j)/\hbar$. By assuming that all intermediate levels are far from resonance, we can transform Eq. (1) into the frequency domain, obtaining for nonresonant transitions [2]

$$P_{\rm nr}^{(3)}(\omega)\propto\int_0^\infty d\omega_1\int_0^\infty d\Omega\,\epsilon_{\rm pr}(\omega-\Omega)$$
$$\times\epsilon_s^*(\omega_1-\Omega)\epsilon_p(\omega_1), \quad (2)$$

whereas for a singly resonant Raman transition through an intermediate level $|i\rangle$ at an energy of $\hbar\omega_R$ and a bandwidth Γ, we obtain

$$P_r^{(3)}(\omega)\propto\int_0^\infty d\omega_1\int_0^\infty d\Omega\,\epsilon_{\rm pr}(\omega-\Omega)$$
$$\times\frac{\epsilon_s^*(\omega_1-\Omega)\epsilon_p(\omega_1)}{(\omega_R-\Omega)+i\Gamma}. \quad (3)$$

Most importantly, since the level lifetimes are in the picosecond range, the spectral content of femtosecond pulses is much larger than Γ. Phase-only pulse shaping, used in our experiments, simply means multiplication of one or more of the electric fields in Eqs. (2) and (3) by a phase function $\exp[i\Phi(\omega)]$.

As is evident from Eq. (2), the nonresonant signal is maximized by transform-limited pulses at zero relative delay. Being a convolution of three pulses, it decays when the relative delay is of the order of the pulse length. The resonant signal, however, exhibits two significantly different behaviors. (a) Since the resonant signal is strongly weighted on $\Omega\approx\omega_R$, the signal intensity does not decrease significantly upon application of spectral phase functions $\Phi_p(\omega)$ and $\Phi_s(\omega)$ on the pump and Stokes pulses, respectively, if both functions are slowly varying relative to Γ and

$$\Phi_p(\omega)=\Phi_s(\omega-\omega_R). \quad (4)$$

In the case of impulsive stimulation, i.e., when the Raman band lies within the bandwidth of a single pulse, as in Weiner *et al.*'s [1] experiment, this is equivalent to applying a phase function which is periodic in ω_R. (b) When the probe beam is delayed, the resonant signal intensity decays at the vibrational level lifetime rather than the pulse length.

Quantum beats occur when two resonant levels lie within the bandwidth of the probe pulse [8]. In this case, the population at each level decreases according to its own lifetime, but the relative phase between the two occupied levels is periodic in $\omega_{R1}-\omega_{R2}$. Since the observed signal is a coherent sum of the two excitations, a beating at this characteristic frequency will be observed. The beat amplitude can serve as a means to measure the relative occupations of the two levels.

In our experiments, the CARS process involves three exciting pulses: A Ti:sapphire mode locked laser (Spectra Physics Tsunami, 80 MHz repetition rate) at 810 nm (150 mW average power) serving as the probe beam, and both the signal and the idler beams of an optical parametric oscillator (Spectra Physics Opal, pumped by the Ti:sapphire laser) centered at about 1500 nm (40 mW average power) and 1760 nm (10 mW average power), serving as the pump and Stokes beams, respectively. All beams have a bandwidth of about 120 $\rm cm^{-1}$, corresponding to 100 fs nearly transform-limited pulses. The spectral phase of both the pump and Stokes pulses is controlled by Fourier-transform pulse shaping [1,2] using a programmable liquid-crystal Spatial Light Modulator (SLM) (CRI SLM-128), half of which is allocated for each of the two beams. The shaper enables both correction of the dispersion in each beam and application of any desired phase function. The spectral resolution is determined by the pixels of the SLM, about 5 $\rm cm^{-1}$ for the pump beam and about 3.5 $\rm cm^{-1}$ for the Stokes beam. Note that this limitation is rather restrictive when attempting to impose phase functions according to Eq. (4), since the spectral resolutions of the pump beam and the Stokes beam are different. Therefore, we apply only rather simple phase functions in the experiments described below. This restriction could be relaxed using holographic phase masks rather than a SLM. The probe beam remains transform-limited. The three beams are spatially and temporally overlapped in a collinear configuration using dichroic beamsplitters and two variable delay lines. The overlapped beams are then focused into the sample using an $NA=0.2$ objective. The CARS signal, collected using a similar numerical aperture lens, is filtered by a bandpass filter and measured with a photomultiplier tube (PMT) and a lock-in amplifier. An outline of the experimental setup is presented in Fig. 1(a).

We first demonstrate coherent control of the CARS process using the 992 $\rm cm^{-1}$ line of benzene. The CARS signal intensity as a function of the probe delay in the case of three transform-limited pulses is shown in Fig. 2(a). The sharp peak around zero delay is due to the nonresonant interaction, while the slowly decaying part is the resonant signal. Since the model calculates separately both the resonant and the nonresonant contributions, and only then sums them up coherently, we can infer from it that at zero relative delay both are almost equal in magnitude. We modulate the phase of both the pump and Stokes using rectangular step phase functions $\Phi_{p/s}(\omega)=\pi\,\mathrm{rect}[(\omega-\omega_0^{p/s})/d]$. In all experiments, we fix ω_0^p, while scanning ω_0^s. This simple phase function is schematically plotted in Fig. 1(c). Note that this is a real

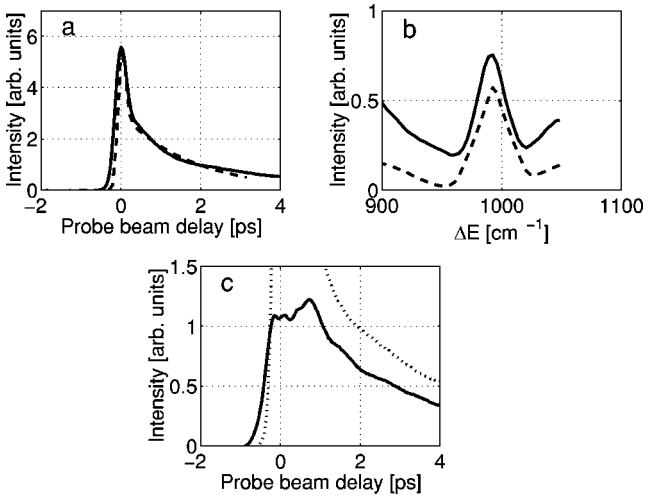

FIG. 2. CARS signals from a benzene sample: (a) Intensity as a function of the probe delay for transform-limited pulses (experiment, solid line; model, dashed line). (b) Intensity as a function of the energy difference between the pump and Stokes phase steps at zero probe delay (experiment, solid line; model, dashed line). (c) Intensity as a function of the probe delay with pump and Stokes shaped to minimize the nonresonant signal while retaining the resonant signal (solid line) compared with the transform-limited signal of (a) (dotted line).

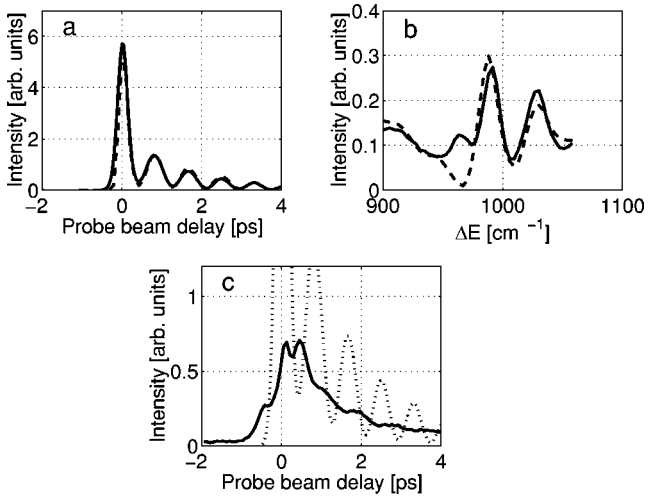

FIG. 3. CARS signals from a pyridine sample: (a) Intensity as a function of the probe delay for transform-limited pulses (experiment, solid line; model, dashed line). (b) Intensity as a function of the energy difference between the pump and Stokes phase steps at 1 ps probe delay (experiment, solid line; model, dashed line). (c) Intensity as a function of the probe delay with pump and Stokes shaped to minimize the 1028 cm^{-1} level population, while retaining the 988 cm^{-1} level population (solid line) compared with the transform-limited signal of Fig. 3(a) (dotted line).

function, merely inverting the sign of the electric field at a given energy range. The experimental results of such a scan, using a $d=30$ cm^{-1} step width, are plotted in Fig. 2(b), along with the theoretical predictions of Eqs. (2) and (3). The CARS signal is greatly reduced when the energy spacing of the applied phase function $\Delta E=\hbar(\omega_0^p-\omega_0^s)$ does not correspond to the excited vibrational level, and is reconstructed when $\Delta E=\hbar\omega_R$. Using an optical spectrum analyzer (Ando AQ-6315) to measure the exact locations of the imposed phase steps, it is possible to obtain a value of 990 ± 5 cm^{-1} for the Raman level energy. Note that since the scan is taken at zero relative delay of the probe beam, the resonant peak lies within some nonresonant background. As can be seen in Fig. 2(b), at the peak of the Raman level, the nonresonant background signal is reduced to a smaller amplitude than the resonant signal, in contrast with the nearly equal magnitude signals obtained at zero relative delay for transform-limited pulses. This is due to the fact that the sum over the different paths in Eq. (2) contains terms with an opposite sign upon application of a phase step on the pump and Stokes pulses. As the phase steps width d is increased continuously from zero, the nonresonant signal amplitude decreases. Since we are limited by the pulse shaper resolution, we slightly decrease the relative phase of the steps from π, and compare in Fig. 2(c) the CARS signal as a function of the probe delay for 0.8π phase steps ($d=30$ cm^{-1}) at the peak of the resonant Raman signal in Fig. 2(b), with the transform-limited signal. As can be seen, while the nonresonant signal has been reduced by an order of magnitude relative to the transform-limited case, the resonant signal was only reduced by about 30%. Thus, the generated pulse is, in essence, a ''dark pulse'' for nonresonant transitions [2].

Selectivity of Raman levels by coherent control can be achieved in a manner similar to the reduction of the nonresonant signal. We look at two Raman levels of pyridine, at 988 cm^{-1} and at 1028 cm^{-1}. Both levels have a similar cross section and a bandwidth of about 2.2 cm^{-1}. The energy difference between these two levels has been measured experimentally from the quantum beats between the two levels [8]. Such beats are shown in Fig. 3(a). The only (limited) control over the relative population of each level was by changing the energy difference between the central wavelengths of the pump and Stokes pulses. In this case, the population of the 988 cm^{-1} level is somewhat higher. In Fig. 3(b), we demonstrate the selective population of either of the two levels. We show again a scan of a $d=25$ cm^{-1} phase step. In this case, the probe delay was set to 1 ps, in order to eliminate the nonresonant background. The measured Raman level energies of the two peaks are 985 ± 5 cm^{-1} and 1027 ± 5 cm^{-1}, respectively. By positioning the phase step at each of the two peaks of Fig. 3(b), it is possible to populate preferentially that level. This is verified by measuring the quantum beat amplitude. In Fig. 3(c), we fix the phase function on the 988 cm^{-1} level. As can be seen, the quantum beat amplitude is reduced by almost an order of magnitude as compared with the transform-limited signal, implying a nearly exclusive population of this Raman level, while the decrease in the 988 cm^{-1} level population relative to the transform-limited case is only about 30%. Note also that the phase of the beats is inverted, indicating an inverted relative phase of the level populations. Since this phase is both real and continuous in the step width d, fixing the phase step width at a somewhat lower value would have resulted in complete elimination of the 1028 cm^{-1} level population.

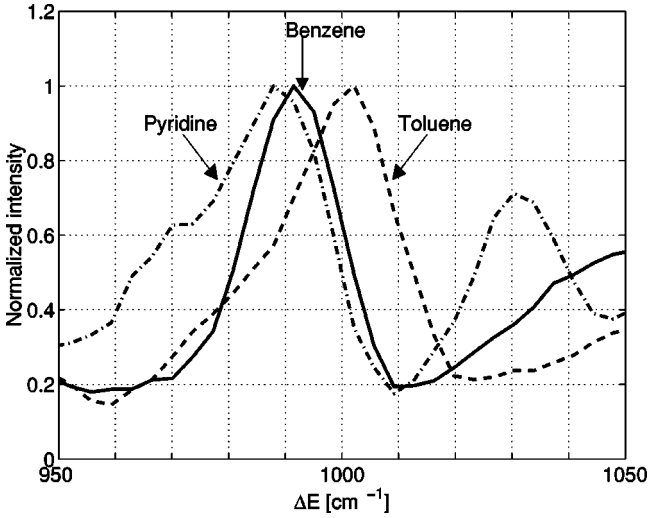

FIG. 4. Comparison between three aromatic compounds (benzene, solid line; toluene, dashed line; pyridine, dash-dotted line) of the intensity as a function of the energy difference between the pump and Stokes phase steps at 0.5 ps probe delay.

We are not only able to selectively excite a given Raman energy level, but also to obtain high spectral resolution of the Raman levels. This is demonstrated by comparing the Raman spectra, as obtained by scans of a $d=15\ \mathrm{cm}^{-1}\pi$ phase step on three different aromatic liquids: benzene ($992\ \mathrm{cm}^{-1}$), toluene ($1001\ \mathrm{cm}^{-1}$), and pyridine (988 and $1028\ \mathrm{cm}^{-1}$). As can be seen in Fig. 4, the differences in the peak locations are distinct, and are in agreement with the known values of these Raman levels. Note that a narrow phase step was used for high-resolution spectroscopy, whereas a wider one was used to eliminate the nonresonant signal. These can be simultaneously achieved by using a more complex phase function with narrow internal structure, stretched over a wider band (for example, a number of narrow phase steps).

In summary, we have demonstrated how through the application of very simple phase functions on the excitation pulses, near complete control of the CARS process can be achieved, enabling the selective population of a given Raman level. By exploitation of the spectral phase correlations of the exciting pulses, we can achieve selectivity with a resolution smaller by almost an order of magnitude than the excitation pulses bandwidth.

The ability to selectively steer the CARS process through a given transition while eliminating the nonresonant background noise could most dramatically affect nonlinear CARS microscopy, where selective imaging of a sample with a weak Raman transition or at lower concentrations could be achieved.

Financial support by the Israel Science Foundation and by the German BMBF is gratefully acknowledged.

[1] A.M. Weiner, D.E. Leaird, G.P. Wiederrecht, and K.A. Nelson, J. Opt. Soc. Am. B **8**, 1264 (1991).
[2] D. Meshulach and Y. Silberberg, Phys. Rev. A **60**, 1287 (1999).
[3] N. Dudovich, B. Dayan, S.M. Gallagher Faeder, and Y. Silberberg, Phys. Rev. Lett. **86**, 47 (2001).
[4] D. Meshulach, D. Yelin, and Y. Silberberg, Opt. Commun. **138**, 345 (1997).
[5] A. Assion, T. Baumert, M. Bergt, T. Brixner, B. Kiefer, V. Seyfried, M. Strehle, and G. Gerber, Science **282**, 919 (1998).
[6] T.C. Weinacht, J.L. White, and P.H. Bucksbaum, J. Phys. Chem. A **103**, 10 166 (1999).
[7] *Infrared and Raman Spectroscopy*, edited by B. Schrader (VCH, Weinheim, 1995).
[8] R. Leonhardt, W. Holzapfel, W. Zinth, and W. Kaiser, Chem. Phys. Lett. **133**, 373 (1987).
[9] A. Zumbusch, G.R. Holtom, and X.S. Xie, Phys. Rev. Lett. **82**, 4142 (1999).
[10] M. Muller, J. Squier, C.A. de Lange, and G.J. Brakenhoff, J. Microsc. **197**, 150 (2000).
[11] M. Hashimoto, T. Araki, and S. Kawata, Opt. Lett. **25**, 1768 (2000).
[12] M.D. Levenson, *Introduction to Nonlinear Laser Spectroscopy* (Academic Press, New York, 1982), p. 136.
[13] J.J. Song, G.L. Eesley, and M.D. Levenson, Appl. Phys. Lett. **29**, 567 (1976).